Title
A PROPOSED ORBIT AND VERTICAL DISPERSION CORRECTION SYSTEM FOR PEP

Author
Close, E.

Publication Date
1978-07-01

Presented at the Particle Accelerator
Conference, San Francisco, CA,
March 12-14, 1979

LBL-9068
PEP Note-271

C.2

A PROPOSED ORBIT AND VERTICAL DISPERSION CORRECTION SYSTEM FOR PEP

E. Close, M. Cornacchia, A. S. King, M. J. Lee

July 1978

Prepared for the U. S. Department of Energy
under Contract W-7405-ENG-48

DISCLAIMER

PEP Note - 271
July 1978

A PROPOSED ORBIT AND VERTICAL DISPERSION CORRECTION SYSTEM FOR PEP

E. Close, M. Cornacchia, A. S. King, M. J. Lee

1. ABSTRACT

The proposed arrangement of position monitors and dipole magnets for the closed orbit correction system in PEP is described. The computer code ALIGN, which simulates and corrects closed orbit displacements, has been used to study the most effective layout of monitors and correctors. The vertical dispersion function has been computed before and after closed orbit correction. The results indicate that the residual vertical dispersion after the orbit is corrected could exceed the tolerable values. A correction procedure for the vertical dispersion has been studied with the computer code CO-OP and this scheme of correction has been verified experimentally in SPEAR.

2. ORBIT AND DISPERSION BEFORE CORRECTION

The closed orbit distortions due to magnet field errors and misalignments were simulated with the computer program ALIGN, as described in Appendix A. Survey misalignments and field errors were chosen randomly out of gaussian distributions with the following r.m.s. values:

Vertical misalignments of quadrupoles	0.2 mm
Horizontal misalignments of quadrupoles	0.2 mm
Relative field error in dipoles	1×10^{-4}
Misalignment errors of secondary monuments	0.3 mm
Misalignment errors of major monuments	20 μrad

The lattice configuration used was a standard PEP lattice with $\nu_x = 21.23$; $\nu_y = 18.67$; $\beta_y^* = 0.11$ m; $\beta_x^* = 2.88$ m; $\eta_x^* = -0.468$ m, where a * denotes the interaction point values. Table 1 gives the values of the uncorrected orbits and vertical dispersion: they are computed at 1044 "stations" around the ring (namely, at the mid-points of every

quadrupole, dipole, sextupole, beam position monitor, dipole corrector). The r.m.s. values are calculated over 20 "machines", each with a random selection of misalignments and field errors.

Table 1

Uncorrected Closed Orbits

$\langle\langle y_c^2 \rangle\rangle$	$\langle \hat{y}_c^2 \rangle^{1/2}$	$\langle y_c^2 \rangle^{1/2}_{I.P.}$	$\langle\langle \eta_y^2 \rangle\rangle^{1/2}$	$\langle \hat{\eta}_y^2 \rangle^{1/2}$
15.2	88.6	1.0	525	2637

$\langle \eta_y^2 \rangle^{1/2}_{I.P.}$	$\langle\langle x_c^2 \rangle\rangle^{1/2}$	$\langle \hat{x}_c^2 \rangle^{1/2}$	$\langle x_c^2 \rangle^{1/2}_{I.P.}$
18	6.5	25.7	2.9

y_c, vertical closed orbit, x_c, horizontal closed orbit, η_y, vertical dispersion, are expressed in mm. The symbol $\langle\langle\ \rangle\rangle$ denotes r.m.s. over 20 machines; $\langle \hat{\ } \rangle^{1/2}$ signifies r.m.s. of the maximum value in each machine, over 20 machines. $\langle\ \rangle^{1/2}_{I.P.}$ are the values calculated at the interaction points.

Because of the large value of the vertical β function at the location of the quadrupoles adjacent to the interaction point (940 m, as compared to the average ~30 m outside the interaction region), most of the contribution to the displaced vertical orbit comes from the misalignment of these quadrupoles. Under this assumption, the r.m.s. of the vertical orbit at the high β_y quadrupole location (or, which is the same, the r.m.s. of the maximum orbit displacement) is:[1]

$$\langle \hat{y}_c^2 \rangle^{1/2} = \beta_y \left(\frac{g\ell}{B\rho}\right) \frac{\sqrt{N}}{2 \sin(\pi\nu_y)} \langle d^2 \rangle^{1/2} \qquad (1)$$

with β_y = 940 m

$\frac{g\ell}{B\rho}$ = integrated quadrupole strength = 0.215 m^{-1}

N = number of high β_y quadrupoles = 12

$\langle d^2 \rangle^{\frac{1}{2}}$ = r.m.s. of vertical displacement = 0.2 mm

ν_y = vertical tune = 18.67

With the above data, we get $\langle \hat{y}_c^2 \rangle^{\frac{1}{2}}$ = 81 mm, in good agreement with the computer result given in Table 1 (89 mm).

3. THE HARMONICS BEFORE ORBIT CORRECTION

Fig. 1a shows the spectrum of the normalized vertical closed orbit before correction for one particular "machine". As expected, the harmonics close to the tune (= 18.67) are strongly dominant. Fig. 2a shows the harmonic content of the vertical dispersion for the same machine. The theoretical expression of the vertical dispersion is given in Appendix C. Let's write it in the form of a harmonic series:

$$\bar{\eta}_y = \sum_{\ell=-\infty}^{\infty} \frac{d_\ell e^{i\ell\phi_y}}{\ell^2-\nu_y^2} \quad , \tag{2}$$

where the bar denotes values normalized to the square root of the beta function, and

$$d_\ell = \frac{1}{2\pi} \int_{-\pi}^{\pi} (D-A\bar{\eta}_x)\, \bar{y}_c\, e^{-i\ell\phi_y}\, d\phi_y \; . \tag{3}$$

The terms D and A are related to the quadrupole and sextupole strengths, respectively (see Appendix C); ϕ_y is the vertical betatron phase divided by the machine tune; $\bar{y}_c$ is the vertical closed orbit, which can be written as

$$\bar{y}_c = \sum_{k=-\infty}^{\infty} \frac{f_k\, e^{ik\phi_y}}{k^2-\nu_y^2} \quad , \tag{4}$$

with

$$f_k = \frac{-1}{2\pi} \int_{-\pi}^{\pi} \nu_y^2 \beta_y^{3/2} \frac{\Delta B_x}{B\rho} e^{-ik\phi_y}\, d\phi_y \; . \tag{5}$$

The vertically deflecting dipole fields, ΔB_x, resulting from displaced quadrupoles have the biggest effect on $\bar{y}_c$. If the quadrupole misalignments are uncorrelated, all the harmonics of the field errors have equal weight, and the closed orbit specturm has a peak at the harmonic closest to the tune, as shown in Fig. 1a. By combining Eqs.(2) and (3), the vertical dispersion can be written as

$$\bar{\eta}_y = \frac{1}{2\pi} \sum_{\ell=-\infty}^{\infty} \sum_{k=-\infty}^{\infty} \frac{e^{i\ell\phi_y}}{\ell^2-\nu_y^2} \frac{f_k}{k^2-\nu_y^2} \int_{-\pi}^{\pi} (D-A\bar{\eta}_x)\, e^{i(k-\ell)\phi_y}\, d\phi_y \; . \tag{6}$$

The main contribution to the vertical dispersion comes from the harmonics

$$\ell = \pm m;\; k = \pm m \text{ and } k-\ell = nP$$

where P is the machine periodicity (=6), and n an integer. m is the integer nearest to the vertical tune. For $k=\ell$, the integrand in 6) is proportional to the machine chromaticity. If the latter is perfectly compensated (i.e., equal to zero), its contribution to the vertical dispersion is zero. For $k=-\ell$, the integrand in 6) is proportional to the width of the 1/2 integer resonance $2\nu_y = 2\ell$ or, which is the same, to the amplitude of the β_y function perturbation. Suzuki[2], who has carried out a similar analysis, concluded that a tune close to the systematic 1/2 integer resonance $2\ell = nP$ should be avoided. We agree with this statement, as far as the uncorrected closed orbit is concerned; after correction, as it will be shown later on, the influence of the systematic half-integer resonance is much reduced. Fig. 2a shows that the 19th (closest to the tune), 13th (=19-6) and 25th (=19+6) harmonics

clearly stand out, as expected.

4. CORRECTION OF THE CLOSED ORBIT

We have adopted the correction procedure already used at the ISR and at SPEAR[3]. The method is described in Appendix A: out of a given number of correctors, m, the computer program chooses the n most effective (n<m) in minimizing the r.m.s. of the orbit distortions. There is no reason why one should not use all the available correctors; however, the method works even if n<m; this is shown in Fig. 3, where we plot, for one "machine", the decrease in vertical closed orbit distortion and the vertical dispersion as a function of the number of correctors used (out of a total of 48).

In the proposed system, ninety-six beam position monitors (in each plane) will be initially installed in PEP. In order to find the best locations, the computer program ALIGN was run for many "machines" (usually 20) and the results of the same set of machines for different configurations of monitors and correctors were compared. It was found, not suprisingly, that the best results in terms of residual closed orbit distortions and correctors strengths were obtained when monitors and correctors are reasonably equally spaced in betatron space. What is surprising, and not completely understood, is the dependence of the relative position of monitors and correctors: in a statistically significant number of cases, the smallest residual orbit and minimum corrector strengths were obtained for those configurations having correctors situated close to position monitors.

Figure 4 describes the layout of the system and Table 2 gives the values of the relevant machine functions at the monitors and correctors in 1/12 of the ring. The pattern is reflected at the symmetry point and is repeated at each superperiod.

Table 2

Beta function and betatron phase values at the positions of monitors and correctors in a half superperiod. 48 correctors

BP = horizontal and vertical beam position monitor
H = horizontal closed orbit corrector
V = vertical closed orbit corrector
I.P. = interaction point
D = distance from interaction point (m)

Element	$\nu_x\phi_x/2\pi$	β_x(m)	$\nu_y\phi_y/2\pi$	β_y(m)	D(m)
I.P.	0	2.88	0	0.11	0.0
BP	0.204	35.35	0.248	837.26	9.670
H,V	0.213	121.93	0.248	641.40	13.225
BP	0.241	70.29	0.277	46.15	36.058
BP	0.424	8.08	0.677	30.01	57.833
V	0.465	15.11	0.692	24.17	60.408
H	0.535	14.22	0.759	28.35	68.763
BP	0.727	10.91	0.864	37.01	86.346
H	1.001	15.62	1.022	27.19	111.813
V	1.037	10.67	1.038	37.06	114.800
BP	1.041	10.38	1.039	38.00	115.046
BP	1.361	10.01	1.216	36.78	143.746
H	1.633	15.26	1.380	26.50	169.213
V	1.671	10.28	1.396	36.24	172.200
BP	1.674	10.00	1.397	37.16	172.446
BP	1.759	31.89	1.497	5.91	181.346

Let's consider first the vertical correctors in Fig. 4. To allow a local correction of the orbit position at the interaction point with a nearly compensated bump, we placed a pair of correctors $\sim 90^0$ (betatron phase) from it. Another pair of correctors placed $\pm 180^0$ from the interaction point would allow a local compensation of the angle. However, for economy reasons, the second corrector has been moved away from this optimum position, and it will be wound on a rectangular frame low field bending magnet. This is not a serious limitation: if the vertical closed orbit is corrected to better than 2 mm at the location of the high beta quadrupole, its maximum angle at the interaction point is less than 0.2 mrad, which is acceptable. The remaining two vertical correctors

are approximately equally spaced and approximately 130^0 apart.

The layout of the horizontal correctors follows a similar pattern. The beam position monitors (one type for horizontal and vertical planes) are, whenever possible, close to a corrector: except for the interaction region, they are approximately 60^0 apart. The computed values of the residual closed orbit and vertical dispersion, when all the available 48 correctors are used, are given in Table 3.

Table 3

Corrected orbits. All 48 correctors are used. R.m.s. over 20 "machines".

Vertical plane. y_c, η_y, and ε (measurement error) are expressed in mm. The corrector's strength, B_c, is expressed in microradians.

$\langle\langle y_c^2\rangle\rangle^{1/2}$	$\langle\hat{y}_c^2\rangle^{1/2}$	$\langle y_c^2\rangle^{1/2}$ I.P.	$\langle\langle \eta_y^2\rangle\rangle^{1/2}$	$\langle\hat{\eta}_y^2\rangle^{1/2}$
0.4	1.4	0.6	105	635
0.5	1.7	0.7	136	806
0.7	2.4	0.7	199	1148

$\langle\eta_y^2\rangle^{1/2}$ I.P.	$\langle\langle B_c^2\rangle\rangle^{1/2}$	$\langle\hat{B}_c^2\rangle^{1/2}$	$\langle\varepsilon^2\rangle^{1/2}$
5	49	123	0
7	53	133	0.5
9	64	158	1.0

Horizontal Plane.

$\langle\langle x_c^2\rangle\rangle^{1/2}$	$\langle\hat{x}_c^2\rangle^{1/2}$	$\langle\langle B_c^2\rangle\rangle^{1/2}$	$\langle\hat{B}_c^2\rangle^{1/2}$	$\langle\varepsilon^2\rangle^{1/2}$
0.4	1.8	63	148	0
0.6	2.2	76	181	0.5
0.9	3.4	107	248	1.0

It is interesting to note that the r.m.s. values of the closed orbit before correction at the interaction points (see Table 1) scale approximately like the square root of the beta function when compared with the rest of the machine. After correction, the r.m.s. value of the orbit around the ring decreases dramatically (a factor of 40 in the vertical plane), whereas at the interaction point it only goes down by a factor of 2. This is a consequence of the correction scheme: in reducing the orbit at the beam position monitors located ±10 m ($\pm 89.3^0$ in betatron phase) from the interaction point, the slope is reduced at this point, while the displacement is relatively unaffected.

5. THE HARMONICS AFTER ORBIT CORRECTION

The harmonic spectra of the residual closed orbit and vertical dispersion have been computed. They are shown in Figs. 1b and 2b for the same machine. It can be seen that the spectrum of the closed orbit is fairly flat, within the statistical fluctuations. The vertical dispersion, even after closed orbit correction, has a peak centered at the integer close to the tune.

After correction, the closed orbit can be represented as

$$\bar{y}_c = \sum_{k=-\infty}^{\infty} g_k \, e^{ik\phi_y} \tag{7}$$

where the coefficients g_k, for a "white" spectrum, have equal probability. Under these conditions the vertical dispersion takes the form:

$$\bar{\eta}_y = \frac{1}{2\pi} \sum_{\ell=-\infty}^{\infty} \sum_{k=-\infty}^{\infty} \frac{e^{i\ell\phi_y}}{\ell^2-\nu_y^2} \, g_k \int_{-\pi}^{\pi} (D-A\bar{\eta}_x) \, e^{i(k-\ell)\phi_y} d\phi_y \tag{8}$$

Thus, the spectrum of the vertical dispersion goes like $1/(\ell^2 - \nu_y^2)$, giving a significant peak at $\ell \sim \nu_y$.

The simple harmonic content of the vertical dispersion suggests that it should be possible to reduce it by acting only on a few dipole correctors.

Fig. 3 indicates that, as the vertical closed orbit distortions decrease, so does the vertical dispersion. Fig. 5 shows the correlation between the r.m.s. values of the corrected (with all the available 48 correctors) vertical closed orbit and of the dispersion for a random sample of 20 "machines".

6. CORRECTION OF THE VERTICAL DISPERSION

It has been observed that the value of the luminosity in SPEAR is reduced when the vertical dispersion is too large. The maximum and the r.m.s. values of the dispersion are 10 to 15 cm and 3 to 4 cm, respectively, for typical operating conditions. Since these, as predicted by ALIGN, can be as large as 80 and 15 cm, respectively, it may be necessary to reduce them in PEP. The possibility of such a correction and its effect upon the vertical closed orbit has been investigated by the computer code CO-OP which uses the same optimization procedure as ALIGN to find a set of N correctors that minimizes $\langle \eta_y^2 \rangle^{\frac{1}{2}}$. The mathematical expressions for the solution are given in Appendix B. Table 4 gives some of the results of the computation for one "machine".

Table 4

η_y correction - vertical closed orbit corrected with 48 elements. Results from one machine.

N_c = number of correctors used for η_y.
$\hat{y}_c$ = maximum vertical closed orbit distortion, in mm.
$\langle y_c^2 \rangle^{\frac{1}{2}}$ = r.m.s. of the orbit, in mm.
$\hat{\eta}_y$ = maximum vertical dispersion, in mm.
$\langle \eta_y^2 \rangle^{\frac{1}{2}}$ = r.m.s. of the vertical dispersion, in mm.
$\hat{B}_c$ = maximum strength of the correctors used for η_y, in μrad.
$\langle B_c^2 \rangle^{\frac{1}{2}}$ = r.m.s. of the correctors strength, in μrad.

N_c	$\langle y_c^2 \rangle^{\frac{1}{2}}$	$\lvert\hat{y}_c\rvert^2$	$\langle \eta_y^2 \rangle^{\frac{1}{2}}$	$\lvert\hat{\eta}_y\rvert$	$\langle B_c^2 \rangle^{\frac{1}{2}}$	$\lvert\hat{B}_c\rvert$
0	0.4	1.1	64	304	0	0
1	0.6	2.1	33	114	15	15
2	0.6	2.1	32	106	9	11
3	0.5	2.0	31	108	7	11
4	0.5	1.3	23	62	10	12
5	0.5	1.3	21	60	9	14
6	0.5	1.4	17	58	8	13
7	0.5	1.5	16	63	8	13
8	0.5	1.5	15	61	9	14

It can be seen that with 8 correctors both $\lvert\hat{\eta}_y\rvert$ and $\langle \eta_y^2 \rangle^{\frac{1}{2}}$ can be reduced by a factor of 5. The effect upon the corrected orbit is small, about a 20% increase. This result is consistent with the observation made in the previous section that only a few correctors are needed to correct η_y, provided that the correction is made after the orbit is corrected.

This procedure of orbit/dispersion correction has been tested in SPEAR. Some of the experimental results are described in Appendix D.

7. SUMMARY

With the proposed monitor/corrector system it has been shown that both horizontal and vertical orbits can be kept below 0.5 mm r.m.s., even allowing for a maximum r.m.s. position measurement error of 0.5 mm.

The vertical dispersion due to orbit errors has been found to be not greater than 15 cm r.m.s. after orbit correction: the operational experience in SPEAR suggests that this value may be too large for PEP so that a correction of η_y may be required. The present study has shown that, with only 8 correctors, it should be possible to reduce the vertical dispersion by a factor of 5. The corrected orbit should be relatively unaffected by this correction.

The orbit/dispersion correction scheme has been tried successfully in SPEAR.

Other effects, like sextupole misalignments, non-zero chromaticity,

rotated quadrupole errors, are discussed in Appendix E. In Appendix F we look at the improvement to be obtained by increasing the number of correctors from 48 to 72.

APPENDIX A The computer program ALIGN.

0. Introduction

The computer program ALIGN[4] has been developed to investigate the correction of closed orbit pertubations that arise from survey alignment and bending field errors. It has been built with modules that reflect the actual physical process being simulated. These modules are basically independent and can be called at any stage of the calculation to perform their task using the data that represent the current system state.

Presently ALIGN has modules to:

1. Calculate closed orbits that arise from a simulation of survey alignment and bending field errors;
2. Calculate the vertical dispersion;
3. Perform a harmonic analysis of the closed orbit or vertical dispersion, using a selected set of sample points;
4. Perform a simulated measurement, including errors, of the closed orbit or vertical dispersion using a set of selected monitors;
5. Calculate magnetic field pertubations needed to correct the closed orbit using a selected set of correctors.

To keep the calculations as simple as possible and to minimize computer usage, ALIGN has been built as a thin lens program. All the required unperturbed lattice functions and parameters are calculated in more general lattice codes such as SINCH[5] or PATRICIA[6], and the needed values of tunes, phases, betatron functions, horizontal dispersion, element spacings and strengths are read in and stored for 1/2 superperiod. ALIGN assumes reflection symmetry and n-fold (n=6 for PEP) symmetry to obtain their definition around the ring.

ALIGN is a two dimensional code that has available the x and y plane values at all times. Since it is a thin lens program, repeated use is

made of the basic formula

$$\delta z_i = \frac{\beta_i^{\frac{1}{2}}}{2 \sin(\pi\nu)} \sum_j \beta_j^{\frac{1}{2}} \left(\frac{\Delta B \ell}{B\rho}\right)_j \cos\left[\nu(\pi - |\phi_i - \phi_j|)\right], \qquad (1)$$

which gives the displacement δz_i at position i as a function of the field errors ΔB occuring at the position j in elements of length ℓ. The field error ΔB results either from a quadrupole of gradient g displaced by an amount d ($\Delta B = g \cdot d$) or to a dipolar field error ΔB.

We assume that in each element the phase and the betatron function β change little throughout the length ℓ. Eq. 1, which is a simplified summation representation of the integral, has proved to be adequate for our calculations.

1. Closed Orbit Due to Survey Errors and Field Errors

The placement of the magnetic elements around the ring is subject to survey errors. Program ALIGN simulates the positioning of magnets in the following way.

Three error classes are considered:

1. individual magnet positional scattering with r.m.s. error σ_1
2. secondary monument random walk errors with r.m.s. error σ_2
3. major monument angular measurement errors with r.m.s. error σ_3.

In all cases the samples are drawn from Gaussian distributions.

The final result of the calculation is to construct a geometric line-of-sight reference line that goes from magnet center to magnet center. To accomplish this ALIGN constructs first a reference line using the secondary monuments. These are survey, or reference, points located inside the ring enclosure. It starts at the first secondary monument, locates the next secondary monument and places it with a transverse positional error Δx drawn from the Gaussian sample with r.m.s. error σ_2. It thus established a line-of-sight reference line L_2 between the two monuments. It then advances from the second secondary monument to the third secondary monument and repeats the above process. This is done through one full superperiod. A schematic representation of this is shown in Fig. 6a, where we have, for simplicity, drawn 4 monuments

between two consecutive interaction points, whereas there are 11 in the real machine. Between the superperiod arcs straight lines are drawn as indicated in Fig. 6a, since there are no secondary monuments in that region.

The fact that the line-of-sight orbit does not close is, at present, unimportant. We place the first and last secondary monuments, 1 and 4 in Fig. 5a, exactly under the major monuments. The major monuments are on the surface exterior to the ring structure. The line-of-sight reference line L_2 represents only the errors in locating the monuments inside the ring structure.

We now establish the line-of-sight reference line L_3 associated with the major monuments. The principal error here is angular, as shown in Fig. 6b. We assume that points 1 and 2 have been established by an angular measurement affected by an error of $\Delta\theta$ r.m.s. value σ_3. To insure closure of L_3 we find the total distance Δx by which it fails to close and then force closure by linearly distributing that error all the way around L_3. The resultant closed reference line is then used as the correct, or survey, reference line.

We now superpose L_2 and L_3 by attaching the first and last secondary monument of each superperiod directly to the major monument line of sight reference line L_3 and then superposing the intermediate points of L_2 on the line L_3. This is shown in Fig. 6c, where, we depict a similar example where the minor monuments 2 and 3 are assumed to be the only ones between the end points 1 and 4. In reality, there are 9 minor and 2 major monuments per 1/2 superperiod.

At this stage of the simulation process we have established a line of sight reference line L_2+L_3 which will be used to place the magnets. We now place the magnetic elements on this line with a magnet to magnet positional error drawn from a Gaussian with r.m.s. error σ_1. The reference line $L_1+L_2+L_3$, shown in Fig. 6d, now passes through the center of each magnetic element.

To obtain the final reference curve passing through all the magnet centers, the program subtracts the 0th and 1st harmonic contributions from the geometric orbit. These correspond in the horizontal plane to a monument error and a translation error, respectively. In the vertical

plane they correspond to a height error and a tilt. Since we do not expect to use the correction elements to compensate for these errors, they are removed from the geometric orbit.

The magnet strengths and ring functions are now used to calculate the closed orbit displacements that arise because the magnets are not on the ideal orbit. Eq. 1 is used for this purpose. The bending field errors $\Delta B/B$ are drawn from a Gaussian sample with r.m.s. error σ_4. The geometric line-of-sight reference curve $L = L_1 + L_2 + L_3$ - (0th har.)-(1st harmonic) is subtracted from the closed orbit to give a resultant displaced equilibrium orbit, DEO, as measured from the magnet centers and their connecting line-of-sight reference lines. It is this final DEO that is used in the program ALIGN at all times.

In the horizontal plane all errors are used and their typical values are:

σ_1 = .2 mm
σ_2 = .3 mm
σ_3 = 20 μrad
σ_4 = 1×10^{-4}

In the vertical plane the reference line is established by means of a liquid level. In this case the only important errors are those caused by vertical misalignments of the quadrupoles, with σ_1 = 0.2 mm.

2. Calculation of the Vertical Dispersion

The vertical dispersion is calculated in ALIGN using Eq. 11 in Appendix C. ALIGN has stored the current displaced equilibrium orbit Y_c at all the stations. It also has stored the values of the horizontal dispersion as input data along with the selected list of magnetic elements and their strengths. Whenever a displaced closed orbit is generated this module will furnish a corresponding value of η_y.

3. Harmonic Analysis

ALIGN computes the Fourier series coefficients (harmonics) of the normalized closed orbits and vertical dispersion. It does this by sampling the selected function at given sample points around the ring

and applying a least square fit of sines and cosines.

4. Simulated Measurements

ALIGN simulates the measurement of orbit positions at some chosen monitors. The measurement errors at the measuring stations (position monitors) are drawn from a Gaussian distribution with a given r.m.s. error. The program superposes the samples on the existing orbit displacements and stores them as a "measured" orbit available for use in other sections of the code.

5. Closed Orbit Corrections

One of the basic modules in ALIGN calculates the corrector strengths needed to correct a displaced equilibruim orbit. The basic equation 1 is used as

$$\delta z = M\theta \tag{2}$$

where

$$M_{ij} = \beta_i^{\frac{1}{2}} \beta_j^{\frac{1}{2}} \cos\left[\nu(\pi - |\phi_i - \phi_j|)\right] / 2 \sin(\pi\nu)$$

$$\theta_j = \left(\frac{\Delta B \cdot \ell}{B\rho}\right)_j \tag{3}$$

$$\delta z_i = \delta x_i \text{ or } \delta y_i \ .$$

The index j runs over the elements chosen as correctors, the index i runs over the stations where the orbit is to be corrected. The 96 position monitors used in the measurement module define the values δz_i of the closed orbit error.

Since there are 48 or 72 correctors for the PEP runs made, we have an overdetermined system and Eq. 2 is solved in a least squares sense for the strengths

$$\theta_j = (\tilde{M}\, M)^{-1}\, \tilde{M}\delta z \tag{4}$$

Although any least squares library subroutine can be used to solve Eq. 2, it has proved advantageous to use a specially modified subroutine MICADO[8], originally written at CERN.

Basically MICADO triangularizes Eq. 2 by means of Householder transformations. However, at each step of this process it checks all the remaining columns in order to determine which column will have, after transformation, the largest pivot at that step. It permutes this column with the current column and then proceeds with the next step. It thus has along the diagonal an ordered set of elements from largest to smallest. This process corresponds to choosing at the k-th step that corrector which has the most significant effect in minimizing the residual when combined with the already chosen k-1 correctors. At any step of the process the current solution can be obtained and convergence criteria monitored. Thus, MICADO allows a more flexible means of choosing effective correctors than do the usual black box least squares solvers. The resultant solution obtained is, nonetheless, the usual unweighted least squares given by Eq. 4.

After obtaining the strengths θ_j, ALIGN used Eq. 1 to construct a correction orbit which it explicitly subtracts from the current DEO to obtain a new, corrected orbit.

6. General Program Structure

The general program structure is shown in the diagram given in Fig. 7.

The control module MO reads a control parameter that selects the task to be done. That task is done in the appropriate module and program control is returned to the driver module MO. Each module communicates with a common area that contains the current system state, in particular all the necessary ring data and the results obtained from other modules. For example, the harmonics of the last harmonic analysis and the current displaced closed orbit are always available. The results of the modules computations are stored in this shared area. Also, subroutines used in many modules are placed in a commonly available subroutine pool. There is, associated with each basic module, an input

module that allows the updating of the module parameters as one of the tasks that can be performed. There is a basic input module MO to initially define the ring.

All modules contain various print options to allow small or large amounts of printout. Each module is self-contained in its x and y parameterization; however, the basic calculation is done using the same coding for both planes.

Assuming that the basic ring data have been loaded, a typical sequence of commands might be:

1	GENX	to generate a x plane orbit
2	MEAX	to measure that orbit
3	CHAX	to correct the orbit
4	MEAX	to measure the corrected x orbit
5	STOP	to stop the program

The program ALIGN is completely task oriented and if we had wished to change the monitors after correction, to look at different or particular orbit positions, we could have inserted

3.1	MEA	read parameters to define monitor points

Further details are available in the program User's Guide.

In the runs that were made for this report an ensemble of 20 machines was typically used and summary tables generated that presented the appropriate r.m.s. values. Each machine is, in principal, statistically independent from the others.

7. Comparison Between ALIGN and PETROS

A study was carried out to check the validity of the approximations involved in ALIGN. The closed orbit distortions and vertical dispersion due to the vertical displacement of one high β_y quadrupole, as computed by the programs ALIGN and PETROS, were compared. PETROS[7] calculates the eigenvalues of the total 5 x 5 transformation matrix which includes coupling.

For a quadrupole displacement of 0.2 mm, the two programs gave the following results:

	$\langle y_c^2 \rangle^{\frac{1}{2}}$	$\lvert\hat{y}_c\rvert$	$\langle \eta_y^2 \rangle^{\frac{1}{2}}$	$\lvert\hat{\eta}_y\rvert$
PETROS	4.60	23.26	202	598
ALIGN	4.20	23.90	212	614

As it can be seen, the agreement between the two programs is rather good.

APPENDIX B

Vertical Dispersion Correction Program (CO-OP)

Let vectors y and η_y be the vertical orbit and dispersion at the position monitors. Let θ be the dipole kicks at the k correctors. Their values are given by:

$$y = y_m + y_c$$

and

$$\eta_y = \eta_{ym} + \eta_{yc} \qquad (1)$$

where m denotes the measured orbit and c the compensations.

If we use the thin lens approximation for the dipole, quadrupole and sextupole magnets, we find

$$y_c = M\theta$$

and

$$\eta_{yc} = N\theta \qquad (2)$$

with the elements of the matrices given by

$$M_{ij} = \frac{\sqrt{\beta_{yi}\,\beta_{yj}}}{2\sin(\pi\nu_y)} \cos\left(\pi\nu_y - |\phi_{yi} - \phi_{yj}|\right) \qquad (3)$$

and

$$N_{ij} = \frac{\sqrt{\beta_{yi}\beta_{yj}}}{2\sin(\pi\nu_y)} \cdot \begin{cases} + \cos(\pi\nu_y - |\phi_i - \phi_j|), \text{ dipoles} \\ + \sum_q \frac{\beta_{yq}(g\ell/B\rho)_q}{2\sin(\pi\nu_y)} \cos(\pi\nu_y - |\phi_{yi} - \phi_{yq}|) \\ \quad \cdot \cos(\pi\nu_y - |\phi_{yi} - \phi_{yj}|), \text{ quadrupoles} \\ - \sum_s \frac{\eta_{xs}\beta_{ys}(2S\ell/B\rho)_s}{2\sin(\pi\nu_y)} \cos(\pi\nu_y - |\phi_{yi} - \phi_{ys}|) \\ \quad \cdot \cos(\pi\nu_y - |\phi_{yi} - \phi_{yj}|), \text{ sextupoles.} \end{cases} \quad (4)$$

In these expressions the strengths of quadrupole and sextupole magnets are given by $g\ell/B\rho$ and $S\ell/B\rho$, ℓ being the magnet length, $B\rho$ the particle rigidity, and β_y, ϕ_y, ν_y the betatron function, betatron phase and the tune. The value of η_{yc} results from

1) The dipole correction (small)
2) The change in orbit at the quadrupole magnets
3) The change in orbit at the sextupole magnets where the horizontal dispersion is different from zero.

CO-OP contains a thin lens version of MAGIC, which calculates lattice solutions for any circular accelerator, and used the optimization procedure MOVQ.[9] For $\langle y^2\rangle^{\frac{1}{2}}$ minimization, the solution is given by

$$\theta_j = -(\tilde{M}\,M)^{-1}\,\tilde{M}y_m \quad (5)$$

as in ALIGN. For $\langle \eta_y^2\rangle^{\frac{1}{2}}$ minimization, the solution is

$$\theta_j = -(\tilde{N}\,N)^{-1}\,\tilde{N}\eta_{ym} \quad (6)$$

In all the computations described in this report, y_m and η_{ym} are the values obtained from ALIGN for a corrected orbit. It is also possible to calculate the correction which minimizes the sum of $f_1 \langle \eta_y^2\rangle$ and $f_2 \langle y^2\rangle$, with weighted factors f_1 and f_2. In our case, however, this feature was not needed, since the correction of $\langle y^2\rangle$ and $\langle \eta_y^2\rangle$, carried out separately, has given satisfactory results.

APPENDIX C

Analytical Expression of the Vertical Dispersion

The expression of the vertical dispersion has been derived by many authors. For clarity, we show how the expression can be obtained. The equation of motion in the vertical plane for an off momentum particle can be written as:

$$y'' + \frac{g}{B\rho}y = -\frac{\Delta B_x}{B\rho}\left(1-\frac{\Delta p}{p}\right) - \frac{2S}{B\rho}xy\left(1-\frac{\Delta p}{p}\right) - \frac{g_r}{B\rho}x\left(1-\frac{\Delta p}{p}\right) + \frac{g}{B\rho}\frac{\Delta p}{p}y \quad (1)$$

S = sextupole strength, defined as $B = S(x^2 - y^2)$
g = main quadrupoles strength
g_r = rotated quadrupoles strength
$\Delta p/p$ = relative momentum deviation
$B\rho$ = magnetic rigidity of the on momentum particle

In the normalized coordinate system of Courant and Snyder[1],

$$\bar{y} = \beta_y^{-\frac{1}{2}}y; \quad \bar{x} = \beta_x^{-\frac{1}{2}}x; \quad \phi_y = \int \frac{ds}{\nu_y\beta_y}.$$

Equation 1 becomes:

$$\frac{d^2\bar{y}}{d\phi_y^2} + \nu_y^2\bar{y} = -\nu_y^2\beta_y^{3/2}\frac{\Delta B_x}{B\rho}\left(1-\frac{\Delta p}{p}\right) - \frac{2S\nu_y^2}{B\rho}\beta_y^2\beta_x^{\frac{1}{2}}\bar{x}\bar{y}\left(1-\frac{\Delta p}{p}\right) + \nu_y^2\frac{g}{B\rho}\beta_y^2\frac{\Delta p}{p}\bar{y} - \frac{g_r}{B\rho}\nu_y^2\beta_y^{3/2}\beta_x^{\frac{1}{2}}\bar{x}\left(1-\frac{\Delta p}{p}\right) \quad (2)$$

Let's take a periodic solution

$$\bar{x} = \bar{x}_c + \bar{\eta}_x \frac{\Delta p}{p}; \qquad \bar{y} = \bar{y}_c + \bar{\eta}_y \frac{\Delta p}{p} \tag{3}$$

where $\bar{x}_c$ and $\bar{y}_c$ are the normalized orbit distortions and $\bar{\eta}_x$ and $\bar{\eta}_y$ the normalized dispersions.

Replacing (3) in (2) and defining

$$A = \frac{2S}{B\rho} \nu_y^2 \beta_y^2 \beta_x^{1/2} \qquad C = \nu_y^2 \beta_y^{3/2} \frac{\Delta B_x}{B\rho}$$

$$D = \nu_y^2 \beta_y^2 g/B\rho \qquad E = \nu_y^2 \beta_y^{3/2} \beta_x^{1/2} \cdot \frac{g_r}{B\rho}$$

we obtain the following two equations for the vertical closed orbit and dispersion, up to first order in $\frac{\Delta p}{p}$:

$$\bar{y}_c'' + \nu_y^2 \bar{y}_c = - A\bar{x}_c\bar{y}_c - C - E\bar{x}_c \tag{4}$$

$$\bar{\eta}_y'' + \nu_y^2 \bar{\eta}_y = - A\bar{\eta}_x\bar{y}_c - A\bar{x}_c\bar{\eta}_y + A\bar{x}_c\bar{y}_c + C + E\bar{x}_c - E\bar{\eta}_x + D\bar{y}_c \tag{5}$$

Retaining only the significant terms ($\bar{\eta}_x\bar{y}_c >> \bar{\eta}_y\bar{x}_c, \bar{x}_c\bar{y}_c$; $\bar{\eta}_x >> \bar{x}_c$), we find

$$\bar{y}_c'' + \nu_y^2 \bar{y}_c \approx -C \tag{4a}$$

$$\bar{\eta}_y'' + \nu_y^2 \bar{\eta}_y \approx -A\bar{\eta}_x\bar{y}_c + C - E\bar{\eta}_x + D\bar{y}_c \tag{5a}$$

Eq. 4a gives the familiar expression of the closed orbit distortion caused by dipole field errors; the main source of errros in PEP is the displacement of the quadrupoles, d, which is seen by a particle as a dipole field B = g·d, superposed to the quadrupole field. Eq. 5a has a Fourier series solution

$$\bar{\eta}_y = \sum_{\ell=-\infty}^{\infty} \frac{d_\ell \, e^{i\ell\phi y}}{\ell^2 - \nu_y^2} \tag{6}$$

with

$$d_\ell = \frac{1}{2\pi} \int_{-\pi}^{\pi} (D - A\bar{\eta}_x) \, \bar{y}_c \, e^{-i\ell\phi_y} \, d\phi_y - \frac{1}{2\pi} \int_{-\pi}^{\pi} E\bar{\eta}_x \, e^{-i\ell\phi_y} d\phi_y \tag{7}$$

The C term on the right hand side of Eq. 5 gives the closed orbit (due to its dependence on momentum); this term is usually small compared to the dispersion ($\bar{\eta}_y >> \bar{y}_c$) and can be neglected.

The normalized closed orbit can be expressed in terms of the dipole field errors:

$$\bar{y}_c = \sum_{k=-\infty}^{\infty} \frac{f_k \, e^{ik\phi y}}{k^2 - \nu_y^2} \tag{8}$$

with

$$f_k = - \frac{1}{2\pi} \int_{-\pi}^{\pi} C \, e^{-ik\phi y} \, d\phi_y \tag{9}$$

Replacing (8) in (7), we obtain

$$d_\ell = \frac{1}{2\pi} \sum_{k=-\infty}^{\infty} \frac{f_k}{k^2 - \nu_y^2} \int_{-\pi}^{\pi} (D - A\bar{\eta}_x) \, e^{i(k-\ell)\phi y} \, d\phi_y + \tag{10}$$

$$- \frac{1}{2\pi} \int_{-\pi}^{\pi} E\bar{\eta}_x \, e^{-i\ell\phi_y} d\phi_y$$

The solution given by Eq. 6, 7 can be expressed in the following alternative form:

$$\bar{\eta}_{yi} = -\frac{1}{2\sin(\pi\nu_y)} \sum_{k=\text{sext}} \left(\frac{2S\ell}{B\rho}\right)_k \beta_{yk}^{1/2}\, \eta_{xk} y_{ck} \cos\left[\nu_y(\pi - |\phi_i - \phi_k|)\right] +$$

$$+\frac{1}{2\sin(\pi\nu_y)} \sum_{k=\text{quads}} \left(\frac{g\ell}{B\rho}\right)_k \beta_{yk}^{1/2}\, y_{ck} \cos\left[\nu_y(\pi - |\phi_i - \phi_k|)\right] + \quad (11)$$

$$-\frac{1}{2\sin(\pi\nu_y)} \sum_{\substack{k=\text{rot}\\ \text{quads}}} \left(\frac{g_r\ell}{B\rho}\right)_k \beta_{yk}^{1/2}\, \eta_{xk} \cos\left[\nu_y(\pi - |\phi_i - \phi_k|)\right] .$$

The integrals in (7) have been replaced by their summation around the ring, in the thin lens approximation; ℓ is the length of the magnetic elements; all the functions on the right hand side of Eq.11 are not normalized to the square root of the beta function.

APPENDIX D.

Correction of Vertical Dispersion in SPEAR

The $\langle\eta_y^2\rangle$ minimization procedure described in Appendix B has been tested experimentally in SPEAR. First, the orbit was corrected and measured, together with the vertical dispersion. The values were then fed into the computer code CO-OP, which predicted the correctors to be used, their strengths, the resultant orbit and dispersion. The computed predicted results are shown in Table 5:

Table 5

η_y correction in SPEAR; computed results. The symbols have the same meanings as in Table 4.

N_c	$\langle y_c^2\rangle^{1/2}$	$\lvert\hat{y}_c\rvert$	$\langle\eta_y^2\rangle^{1/2}$	$\lvert\hat{\eta}_y\rvert$	$\langle B_c^2\rangle^{1/2}$	$\lvert\hat{B}_c\rvert$
0	1.1	1.9	49	95	0	0
1	1.2	2.6	36	117	35	35
2	1.2	2.5	35	106	22	28
3	1.3	2.9	30	92	67	79
4	1.8	4.4	24	57	122	149
5	2.0	4.6	23	57	120	176
6	3.8	11.1	23	55	3760	6590
7	4.5	13.0	23	56	4340	7650
8	4.9	14.0	22	55	4500	6600

The first corrector chosen by the computer code was then energized. The measured values were the following:

$\langle y_c^2\rangle^{1/2}$ = 1.23 mm $\hat{y}_c$ = 2.55 mm

$\langle\eta_y^2\rangle^{1/2}$ = 31 mm $\hat{\eta}_y$ = 76 mm

The repeatibility of the orbit measurements in SPEAR is about ±0.06 mm, which gives a η_y measurement accuracy of ±15 mm. Thus, there is reasonable agreement between measured and computed values (second line in the above table). Increasing the number of correctors did not bring about any further reduction in vertical dispersion, probably because of measurement accuracy. It is interesting to note that in SPEAR the closed orbit distortions after correction increase rapidly with the number of correctors. This may be due to the fact that the 8 correctors in SPEAR are all located in the interaction regions and they are not very effective in correcting the vertical dispersion caused by orbit errors in the sextupole magnets, which are located in the arcs of the machine.

APPENDIX E

Other Effects

a) Non-Zero Chromaticity. It is interesting to compare the contribution to the vertical dispersion due to the quadrupolar and sextupolar terms separately. Over 20 machines, we have:

$\langle\eta_y^2\rangle^{1/2}$ (sext. and quad.)	$\langle\eta_y^2\rangle^{1/2}$ (quad. only)	$\langle\eta_y^2\rangle^{1/2}$ (sext. only)
before closed orbit correction		
0.525 m.	6.271 m.	6.224 m.
after closed orbit correction		
0.105 m.	0.010 m.	0.103 m.

The table shows that, before closed orbit correction, the contributions of the quadrupolar and sextupolar terms are nearly equal: in Eq.(6) of Section 3, the terms for which $k = \ell = m$ cancel out exactly and most of the residual dispersion comes from the terms $k = \ell = -m$, which do not cancel. Also, before closed orbit correction, most of the quadrupolar contribution comes from the high β_y quadrupoles (where the closed orbit attains its maximum values); the effect of the sextupoles, instead, is very much distributed around the ring. After correction, the closed orbit distortions have equal amplitude probability around the ring, regardless of the function values; thus, the relative decrease of the orbit amplitude is much greater at the high β_y quadrupole locations than anywhere else, and the quadrupole dependent vertical dispersion reduction is correspondingly greater. It is of interest to compare the computed results with the theoretical prediction, after closed orbit correction. The vertical dispersion at the i-th location can be written as (considering only the sextupole terms):

$$\eta_{yi} = -\beta_i^{1/2} \frac{1}{2 \sin(\pi\nu_y)} \sum_{k=\text{sext}} \left(\frac{2S\ell}{B\rho}\right)_k \beta_{yk}^{1/2} \eta_{xk} y_{ck} \cos\left[\nu_y(\pi - |\phi_i - \phi_k|)\right] \quad (1)$$

with S = sextupole strength, defined as $B = S(x^2 - y^2)$

y_{ck} = vertical closed orbit at the sextupole location.

The r.m.s. at the high β quadrupole (indicated by $\langle\hat{\eta}_y^2\rangle^{1/2}$) is, for totally uncorrelated orbit displacements,

$$\langle\hat{\eta}_y^2\rangle^{1/2} = \frac{\beta_{y\,\max}^{1/2}}{2 \sin(\pi\nu_y)} \left[\sum_{k=\text{sext}} \left(\frac{2S\ell}{B\rho}\right)^2 \beta_{yk} \hat{\eta}_{xk}^2\right]^{1/2} \langle y_c^2\rangle^{1/2} \quad (2)$$

For PEP the above formula gives:

$\langle\eta_y^2\rangle^{1/2} = 1325 \cdot \langle y_c^2\rangle^{1/2}$; thus, for $\langle y_c^2\rangle^{1/2} = 0.4$ mm., $\langle\hat{\eta}_y^2\rangle_{\text{sext}}^{1/2} = 0.53$ mm.

The computed r.m.s. of the maxima over 20 machines gives:

$$\langle\hat{\eta}_y^2\rangle^{1/2} = 0.63 \text{ m.}$$

From the fact that there is practically no cancellation of quadrupolar and sextupolar terms after closed orbit correction, we can conclude that the effect of a small positive chromaticity (as it may be required by collective effects) on the vertical dispersion is small. Computations have confirmed that a chromaticity of +5. (Chromaticity due to sextupoles only is +165) makes very little difference to the vertical dispersion.

b) Sextupole Misalignments

Eq.(2) tells us that the contribution to the vertical dispersion one can expect from misalignments of the sextupoles. A misaligned sextupole is equivalent to a distorted orbit; if $\langle d^2\rangle^{1/2}$ is the r.m.s. of the distortion, the total dispersion is:

$$\langle\eta_y^2\rangle^{1/2} = 1325 \left[\langle y_c^2\rangle + \langle d^2\rangle\right]^{1/2}$$

Thus, since $\langle y_c^2 \rangle^{\frac{1}{2}} = 0.4$ mm, $\langle d^2 \rangle^{\frac{1}{2}} = 0.2$ mm is an acceptable tolerance since it increases the dispersion by a very small amount.

c) Rotated Quadrupole Errors

In Appendix C we found the following expression:

$$\eta_{yi} = \frac{-\beta_{yi}^{\frac{1}{2}}}{2 \sin (\pi\nu_y)} \sum_{\substack{k=\text{rot} \\ \text{quads}}} \left(\frac{g_r \ell}{B\rho}\right) \beta_{yk}^{\frac{1}{2}} \eta_{xk} \cos \left[\nu_y (\pi - |\phi_i - \phi_k|)\right]$$

g_r is the rotated quadrupole gradient = αg, where α is the angle of rotation in radians and g is the normal gradient. For totally uncorrelated rotations, we have:

$$\langle \hat{\eta}_y^2 \rangle_i^{\frac{1}{2}} = \frac{\beta_{yi}^{\frac{1}{2}}}{2 \sin (\pi\nu_y)} \left[\sum_k \left(\frac{g\ell}{B\rho}\right)^2 \beta_{yk} \eta_{xk}^2\right]^{\frac{1}{2}} \langle \alpha^2 \rangle^{\frac{1}{2}}$$

For PEP, at the location of maximum β_y we have:

$$\langle \hat{\eta}_y^2 \rangle^{\frac{1}{2}} = 302 \langle \alpha^2 \rangle^{\frac{1}{2}}$$

The rotational tolerance is <0.7 mrad r.m.s., giving:

$$\langle \hat{\eta}_y^2 \rangle^{\frac{1}{2}} = 0.217 \text{ m.}$$

This is to be compared to the closed orbit dependent contribution ($\langle \hat{\eta}_y^2 \rangle^{\frac{1}{2}} = 0.63$ m). Since the two values add quadratically, we conclude that the effect of randomly rotated quadrupoles on the vertical dispersion is small compared to the closed orbit effect.

APPENDIX F

Effect of increasing the number of correctors to 72.

A study similar to the one described in Section 4 has been carried out, with the number of correctors increased to 72 in both planes, while keeping the number of beam position monitors fixed at 96. Fig. 8 shows

the proposed layout, and Table 6 gives the computed results. Out of the 72 correctors, only 40 need to be used, as there is very little improvement in increasing the number of iterations in the correction procedure. A comparison with Table 3 (48 correctors) shows that, in terms of closed orbit distortions, there is little to be gained by using a greater number of correctors; it does, however, decreases the vertical dispersion. As the measurement error increases, the difference in performance between the two layouts becomes less significant. Finally, Table 7 shows the results of the correction procedure applied to the 72 correctors layout. The improvement in η_y and the effect on the orbit do not show any striking difference from the 48 corrector case.

Table 6

72 correctors - Corrected orbit - 40 out of 72 correctors are used. R.m.s. over 20 "machines".

Vertical Plane. y_c, η_y and ε (measurement error) are expressed in mm. The correctors strength B_c is expressed in microradians.

$\langle\langle y_c^2 \rangle\rangle^{\frac{1}{2}}$	$\langle \hat{y}_c^2 \rangle^{\frac{1}{2}}$	$\langle y_c^2 \rangle^{\frac{1}{2}}_{\text{I.P.}}$	$\langle\langle \eta_y^2 \rangle\rangle^{\frac{1}{2}}$	$\langle \hat{\eta}_y^2 \rangle^{\frac{1}{2}}$	$\langle\langle B_c^2 \rangle\rangle^{\frac{1}{2}}$	$\langle \hat{B}_c^2 \rangle^{\frac{1}{2}}$	$\langle \varepsilon^2 \rangle^{\frac{1}{2}}$
0.3	1.2	0.5	66	376	54	130	0
0.4	1.6	0.6	111	594	61	141	0.5
0.7	2.4	0.6	190	1038	80	181	1.0

Horizontal plane

$\langle\langle x_c^2 \rangle\rangle^{\frac{1}{2}}$	$\langle \hat{x}_c^2 \rangle^{\frac{1}{2}}$	$\langle\langle B_c^2 \rangle\rangle^{\frac{1}{2}}$	$\langle \hat{B}_c^2 \rangle^{\frac{1}{2}}$	$\langle \varepsilon^2 \rangle^{\frac{1}{2}}$
0.4	1.8	78	179	0
0.6	2.6	98	222	0.5
1.1	4.2	145	328	1.0

Table 7

η_y correction - Vertical closed orbit corrected with 40 correctors chosen from 72 available. Results from one machine. The symbols have the same meanings as in Table 4.

N_c	$\langle y_c^2 \rangle^{\frac{1}{2}}$	$\lvert\hat{y}_c\rvert$	$\langle \eta_y^2 \rangle^{\frac{1}{2}}$	$\lvert\hat{\eta}_y\rvert$	$\langle B_c^2 \rangle^{\frac{1}{2}}$	$\lvert\hat{B}_c\rvert$
0	0.3	0.8	58	260	0	0
1	0.4	1.6	31	105	40	40
2	0.5	2.1	28	88	30	40
3	0.4	1.6	26	67	22	37
4	0.4	1.6	20	49	20	34
5	0.3	0.9	19	60	16	30
6	0.3	0.9	18	56	18	38
7	0.3	1.1	17	49	19	46
8	0.3	1.1	16	48	20	51

ACKNOWLEDGEMENTS

The authors wish to thank H. Wiedemann for his assistance in selecting the locations of monitors and correctors. They are also grateful to B. Autin, A. Garren, P. Morton and R. Sah for useful discussions. The help of H. Schellman and T. Knight in preparing the manuscript is also gratefully acknowledged.

REFERENCES

1. E.D. Courant and H.S. Snyder, Annals of Physics, 3,1-48 (1958).
2. T. Suzuki, PEP-259, November 1977.
3. A.S. King, M.J. Lee, P.L. Morton, IEEE Trans.Nucl.Sci., Vol NS-20, June 1973.
4. LBL/SLAC Alignment Program. Originally started by R. Sah, LBL. Modified and expanded by E. Close.
5. A.A. Garren and A.S. Kenney, LBL Int. Report, 1974.
6. H. Wiedemann, PEP-220, September 1976.
7. PETROS Computer Program, written by K. Steffen at DESY.
8. B. Autin and G. Marti, CERN-ISR-MA/73-17, 1973.
9. SPEAR Orbit Correction Code.

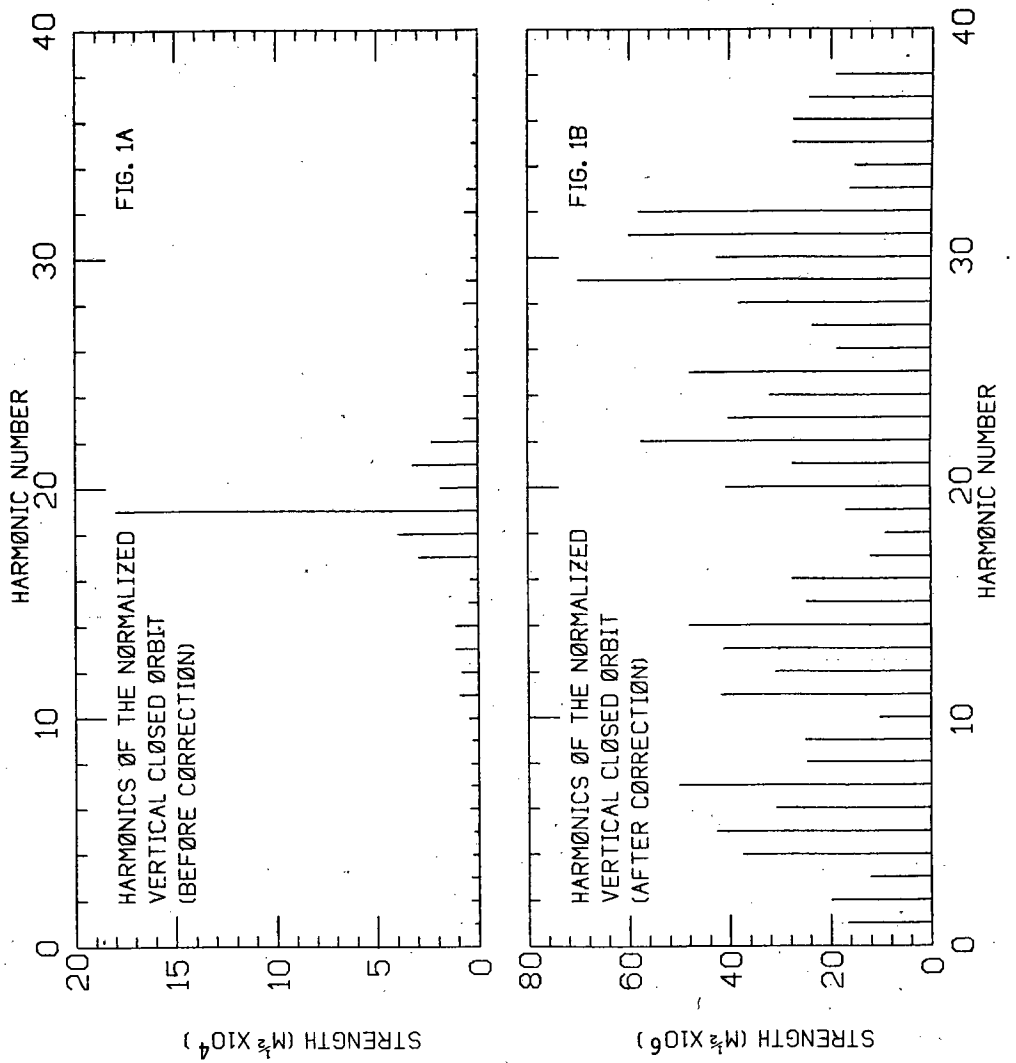

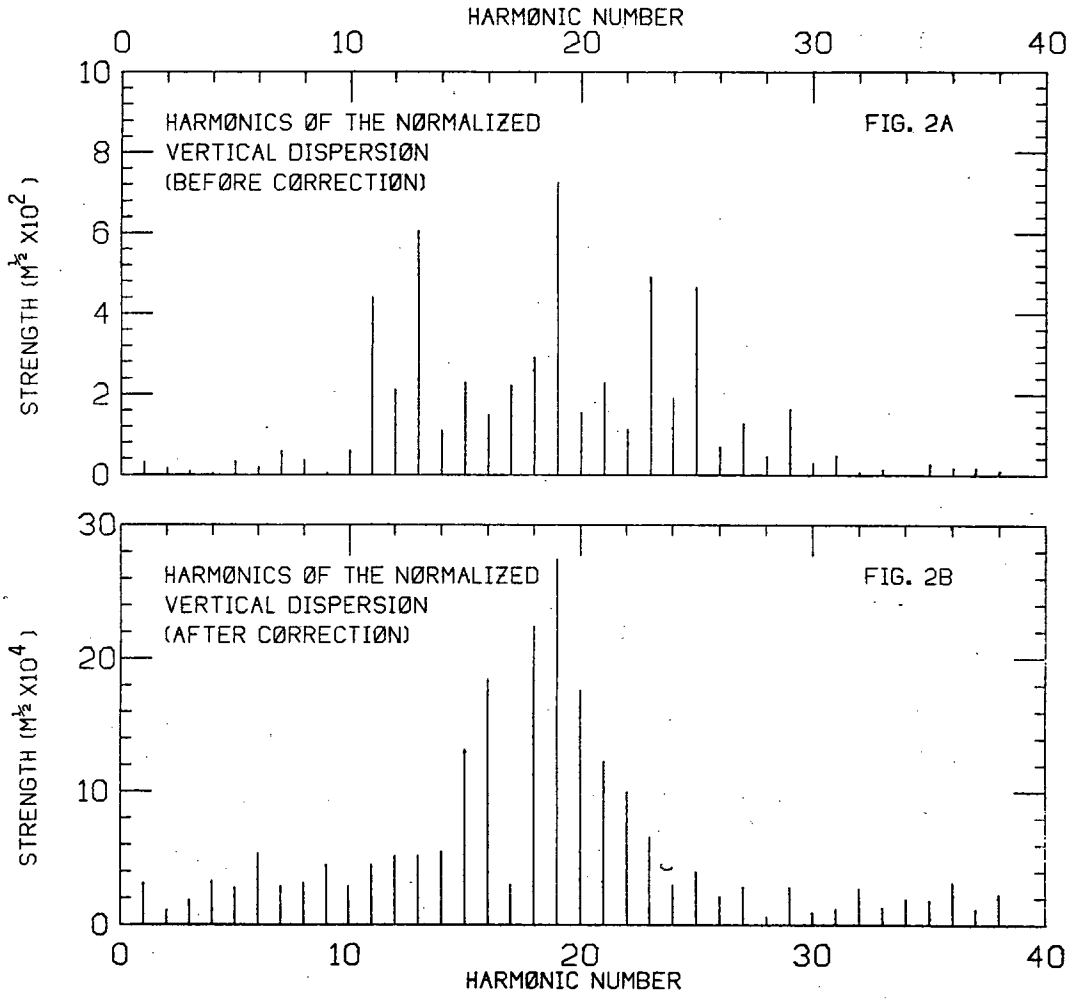
HARMØNIC NUMBER
0
10
20
30
40
HARMØNICS ØF THE NØRMALIZED
VERTICAL DISPERSIØN
(BEFØRE CØRRECTIØN)
FIG. 2A
STRENGTH (M½ X10²)
0
2
4
6
8
10
HARMØNICS ØF THE NØRMALIZED
VERTICAL DISPERSIØN
(AFTER CØRRECTIØN)
FIG. 2B
STRENGTH (M½ X10⁴)
0
10
20
30
HARMØNIC NUMBER

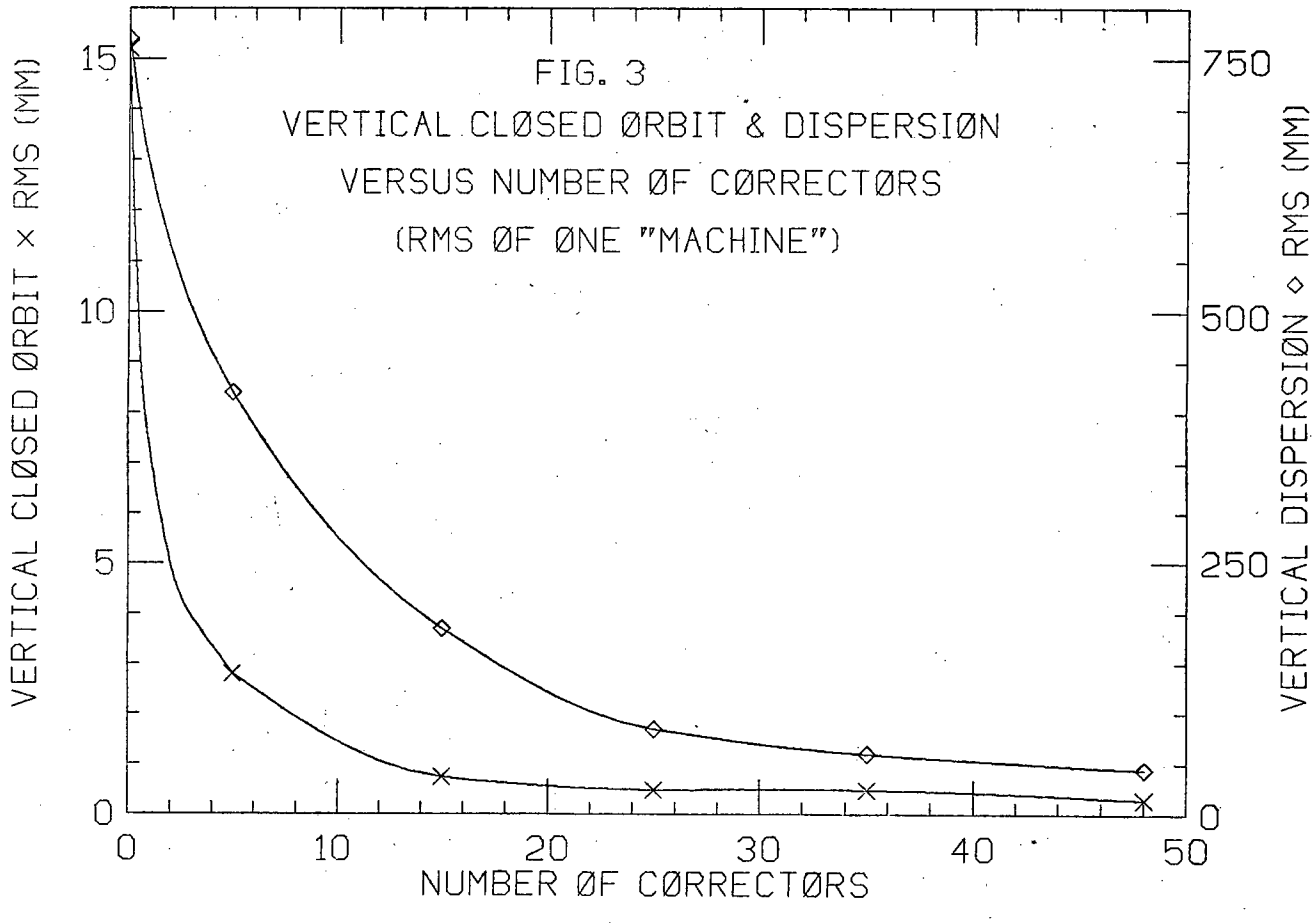
FIG. 3
VERTICAL CLØSED ØRBIT & DISPERSIØN
VERSUS NUMBER ØF CØRRECTØRS
(RMS ØF ØNE "MACHINE")
VERTICAL CLØSED ØRBIT × RMS (MM)
VERTICAL DISPERSIØN ◇ RMS (MM)
NUMBER ØF CØRRECTØRS
0
5
10
15
250
500
750
0
10
20
30
40
50

FIG.4 A LAYØUT ØF A HALF-SUPERPERIØD SHØWING THE RELATIVE PØSITIØN ØF THE PØSITIØN MØNITØRS, DIPØLE CØRRECTØRS, AND THE RING QUADRUPØLE MAGNETS (48 CØRRECTØRS)

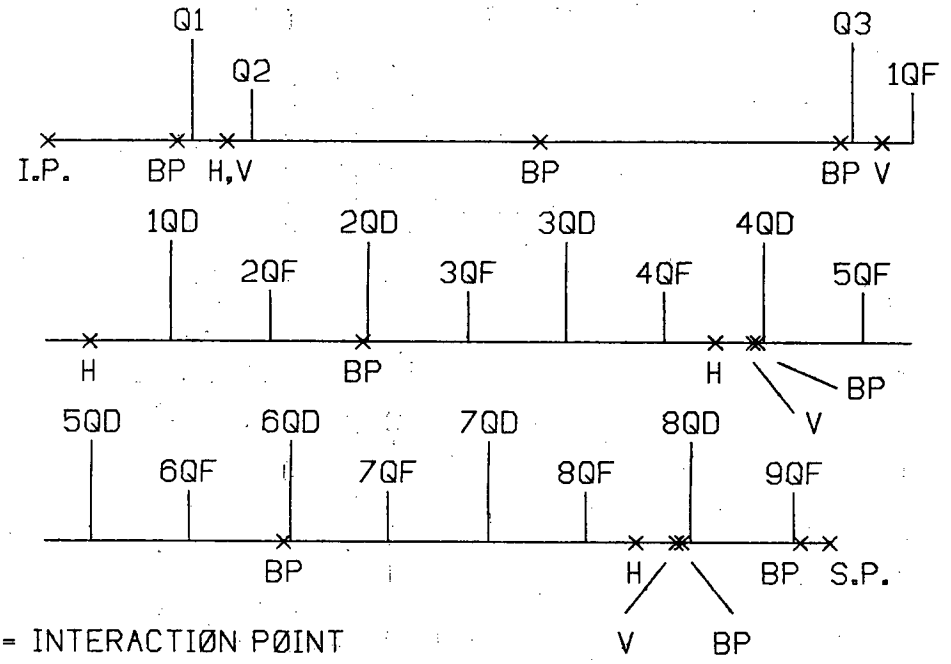

I.P. = INTERACTIØN PØINT
S.P. = SYMMETRY PØINT
BP = BEAM PØSITIØN MØNITØR
Q = QUADRUPØLE MAGNET
H = HØRIZØNTALLY CØRRECTING DIPØLE
V = VERTICALLY CØRRECTING DIPØLE

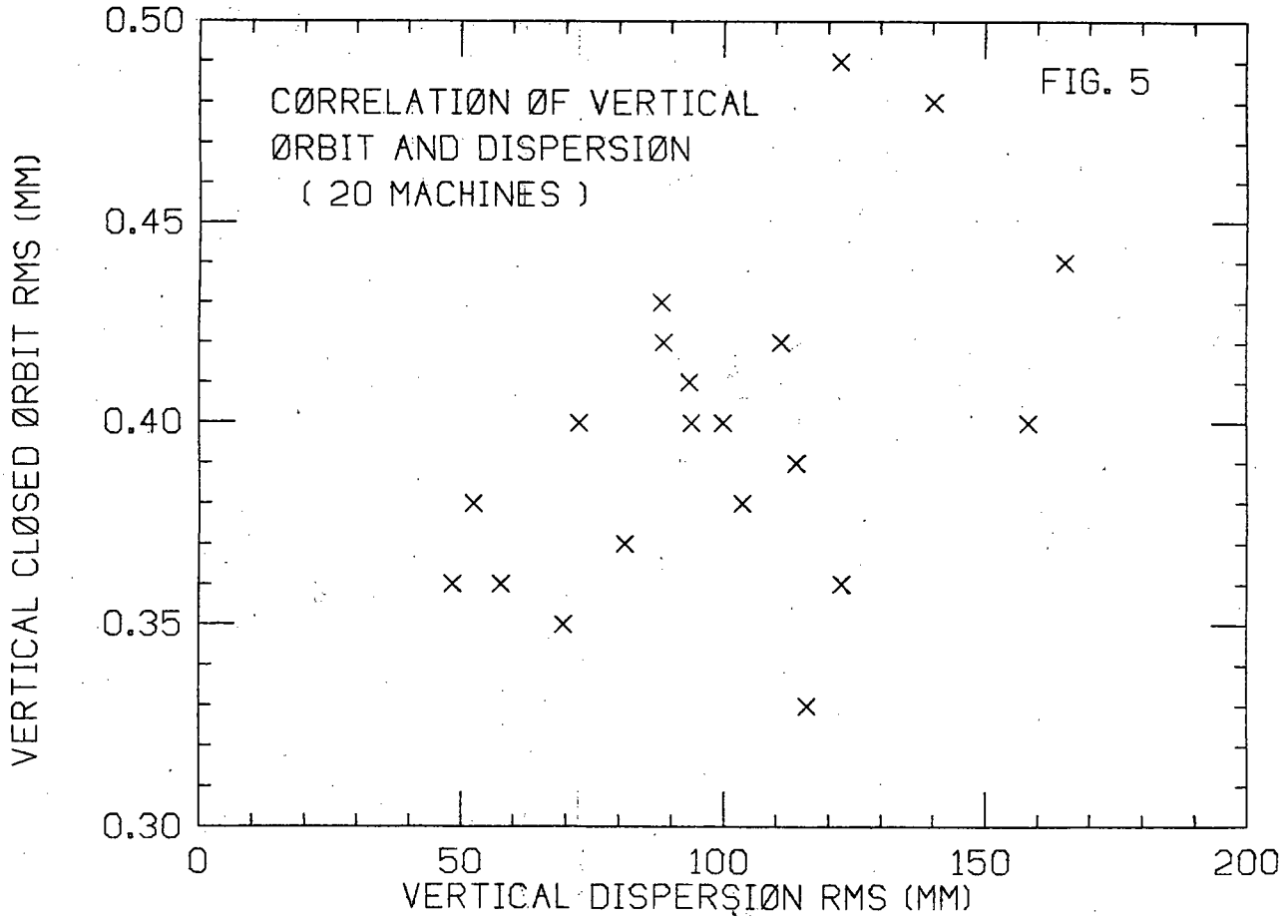

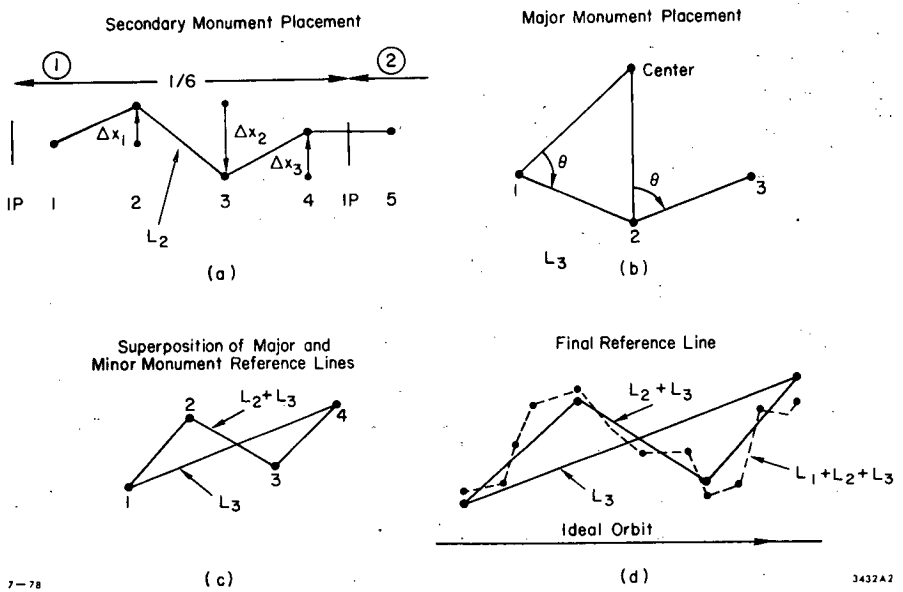
Secondary Monument Placement
1
2
1/6
Δx1
Δx2
Δx3
IP
1
2
3
4
IP
5
L2
(a)
Major Monument Placement
Center
θ
θ
1
2
3
L3
(b)
Superposition of Major and Minor Monument Reference Lines
2
L2+L3
4
1
3
L3
(c)
Final Reference Line
L2 +L3
L1+L2+L3
L3
Ideal Orbit
(d)
7-78
3432A2

Fig. 6

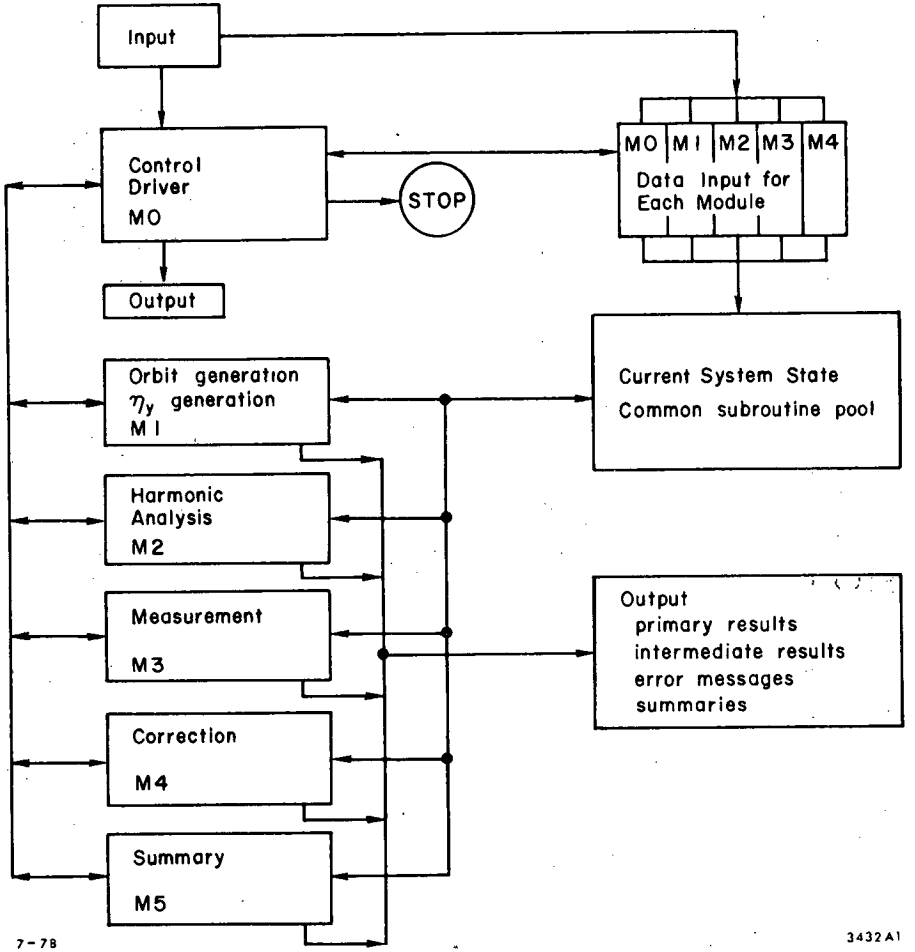
Input
Control
Driver
MO
STOP
MO
M1
M2
M3
M4
Data Input for
Each Module
Output
Orbit generation
η_y generation
M1
Current System State
Common subroutine pool
Harmonic
Analysis
M2
Measurement
M3
Output
primary results
intermediate results
error messages
summaries
Correction
M4
Summary
M5
7-78
3432A1

Fig. 7

FIG.8 A LAYØUT ØF A HALF-SUPERPERIØD SHØWING THE RELATIVE PØSITIØN ØF THE PØSITIØN MØNITØRS, DIPØLE CØRRECTØRS, AND THE RING QUADRUPØLE MAGNETS (72 CØRRECTØRS)

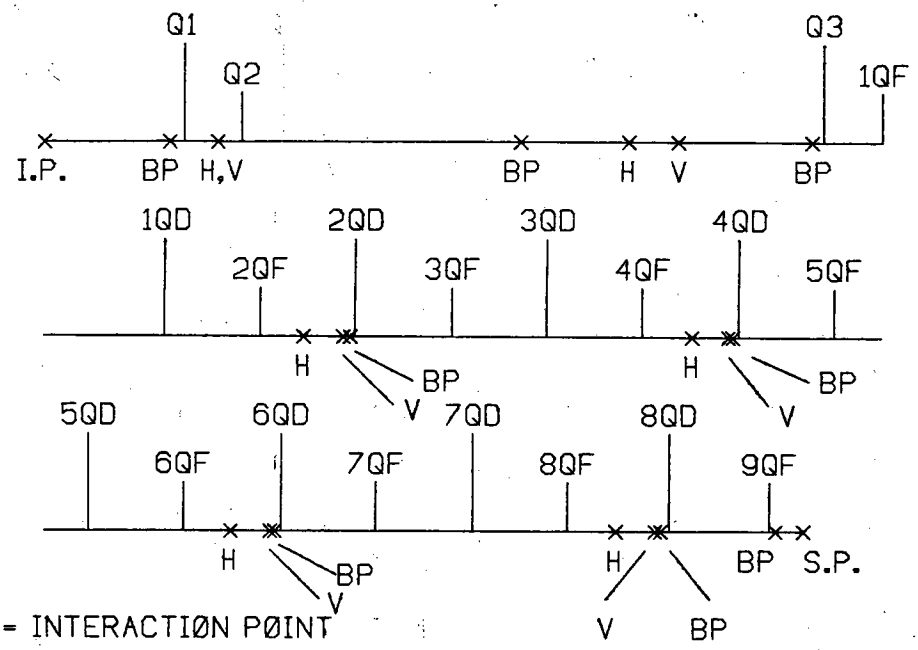

I.P. = INTERACTIØN PØINT
S.P. = SYMMETRY PØINT
BP = BEAM PØSITIØN MØNITØR
Q = QUADRUPØLE MAGNET
H = HØRIZØNTALLY CØRRECTING DIPØLE
V = VERTICALLY CØRRECTING DIPØLE

TECHNICAL INFORMATION DEPARTMENT
LAWRENCE BERKELEY LABORATORY
UNIVERSITY OF CALIFORNIA
BERKELEY, CALIFORNIA 94720